Nuclear symmetry energy and the neutron skin in neutron-rich nuclei

A. E. L. Dieperink,[1] Y. Dewulf,[2] D. Van Neck,[2] M. Waroquier,[2] and V. Rodin[3]
[1]*KVI, Zernikelaan 25, NL-9747AA Groningen, The Netherlands*
[2]*Laboratory of Theoretical Physics, Ghent University, Proeftuinstraat 86, B-9000 Gent, Belgium*
[3]*Institut für Theoretische Physik der Universität Tübingen, D-72076 Tübingen, Germany*
(Received 28 July 2003; published 17 December 2003)

The symmetry energy for nuclear matter and its relation to the neutron skin in finite nuclei is discussed. The symmetry energy as a function of density obtained in a self-consistent Green function approach is presented and compared to the results of other recent theoretical approaches. A partial explanation of the linear relation between the symmetry energy and the neutron skin is proposed. The potential of several experimental methods to extract the neutron skin is examined.

DOI: 10.1103/PhysRevC.68.064307 PACS number(s): 21.10.Gv, 21.30.Fe, 21.65.+f

I. INTRODUCTION

The nuclear symmetry energy plays a central role in a variety of nuclear phenomena. It determines to a large extent the equation of state (EOS) and the proton fraction of neutron stars [1], the neutron skin in heavy nuclei [2], it enters as an input in the analysis of heavy ion reactions [3,4], etc. Its value at nuclear saturation density, $S(\rho_0=0.17\ \mathrm{fm}^{-3}) \approx 30$ MeV, seems reasonably well established, both empirically as well as theoretically; still different parametrizations of relativistic mean-field (RMF) models (which fit observables for isospin symmetric nuclei well) lead to a relatively wide range of predictions for the symmetry energy, 24–40 MeV. However, predictions for its density dependence show a substantially larger variation.

Recently it has been pointed out by several authors [2,5,6] that there exists a strong correlation between the neutron skin, $\Delta R=R_n-R_p$, and the density derivative of the EOS of neutron matter near saturation density. Subsequently in a more detailed analysis in the framework of a mean-field approach, Furnstahl [2] demonstrated that in heavy nuclei there exists an almost linear empirical correlation between theoretical predictions in terms of various mean-field approaches to $S(\rho)$ (i.e., a bulk property) and the neutron skin, ΔR (a property of finite nuclei).

This observation has contributed to a renewed interest in an accurate determination of the neutron skin in neutron-rich nuclei for several reasons. First precise experimental information on the neutron skin could help to further constrain interaction parameters that play a role in the calculation of the symmetry energy [7]. Furthermore a precise value of the neutron skin is required as an input in several processes of physical interest, e.g., the analysis of energy shifts in deeply bound pionic atoms [8], and in the analysis of atomic parity violation experiments (weak charge) [9]. It has been shown that the calculated symmetry energy is quite insensitive to details of modern realistic nucleon-nucleon (*NN*) interactions [10]. On the other hand the symmetry energy and in particular its density dependence can vary substantially with the many-body approximations employed. For instance the results of lowest-order Brueckner-Hartree-Fock (BHF) and variational calculations do not seem to agree well.

The aim of this paper is threefold: First we address the sensitivity of the symmetry energy to various many-body approximations. To this end we present results of a calculation of $S(\rho)$ using the self-consistent Green function (SCGF) approach and compare the result with various other theoretical approaches. Second we will try to provide some new insight in the origin of the "Furnstahl" relation; for this purpose we use the Landau-Migdal effective interaction in the mean-field approximation. Finally in view of the large variety of existing and proposed experimental methods to determine the neutron skin ΔR we examine the merits of some recently proposed methods that seem to be of potential interest to provide more accurate information on the neutron skin in the near future.

Section II is devoted to an overview of theoretical approaches to the symmetry energy, and a new calculation in terms of the self-consistent Green function approach is presented. In Sec. III an interpretation of the Furnstahl relation is presented in terms of the Landau-Migdal approach. Section IV contains an overview of various experimental methods to deduce information on the neutron skin and Sec. V contains a short discussion of implications for other physical processes where the information on the neutron skin is required as an input.

II. THE SYMMETRY ENERGY IN NUCLEAR MATTER

The symmetry energy $S(\rho)$ is defined in terms of a Taylor series expansion of the energy per particle for nuclear matter in terms of the asymmetry $\alpha=(N-Z)/A$ (or equivalently the proton fraction $x=Z/A$),

$$E(\rho,\alpha) = E(\rho,0) + S(\rho)\alpha^2 + O(\alpha^4) + \cdots . \tag{1}$$

It has been shown [11,12] that deviations from the parabolic law in Eq. (1), i.e., terms in α^4, are quite small.

Near the saturation density ρ_0 the energy of isospin-symmetric matter $E(\rho,0)$ and the symmetry energy can be expanded as

$$E(\rho,0) = E_0 + \frac{K}{18\rho_0^2}(\rho-\rho_0)^2 + \cdots , \tag{2}$$

and

$$S(\rho) = \left. \frac{1}{2}\frac{\partial^2 E(\rho,\alpha)}{\partial \alpha^2}\right|_{\alpha=0}$$
$$= a_4 + \frac{p_0}{\rho_0^2}(\rho-\rho_0) + \frac{\Delta K}{18\rho_0^2}(\rho-\rho_0)^2 + \cdots . \quad (3)$$

The parameter a_4 is the symmetry energy at equilibrium and the slope parameter p_0 governs the density dependence.

The relevance of the nuclear matter results in part depends on the question whether there is a surface contribution to the symmetry energy for finite nuclei. In Ref. [13] it was found that the latter is of minor importance, which has also been confirmed in Ref. [2].

A. Self-consistent Green function and Brueckner approach

In this section we describe the calculation of the symmetry energy in the SCGF approach. Since the latter can be considered as a generalization of the lowest-order BHF method we start with a brief discussion of the symmetry energy in the latter case.

1. Symmetry energy in BHF

In the Brueckner-Hartree-Fock approximation, the Brueckner-Bethe-Goldstone (BBG) hole-line expansion is truncated at the two hole-line level. The short-range *NN* repulsion is treated by a resummation of the particle-particle ladder diagrams into an effective interaction or *G* matrix. Self-consistency is required at the level of the BHF single-particle (sp) spectrum $\epsilon^{BHF}(k)$,

$$\epsilon^{BHF}(k) = \frac{k^2}{2m} + \sum_{k'<k_F} \mathrm{Re}\langle kk'|G[\omega = \epsilon^{BHF}(k) + \epsilon^{BHF}(k')]|kk'\rangle . \quad (4)$$

In the standard choice BHF the self-consistency requirement (4) is restricted to hole states ($k<k_F$) only, while the free spectrum is kept for particle states $k>k_F$. The resulting gap in the sp spectrum at $k=k_F$ is avoided in the continuous-choice BHF (ccBHF), where Eq. (4) is used for both hole and particle states. The continuous choice for the sp spectrum is closer in spirit to the many-body Green function perturbation theory. Moreover, recent results indicate [14,15] that the contribution of higher-order terms in the hole-line expansion is considerably smaller if the continuous choice is used.

The BHF energy per nucleon can be easily evaluated for both symmetric nuclear matter (SNM) and pure neutron matter (PNM) using the energy sum rule,

$$\frac{E}{A} = \frac{d}{\rho}\int \frac{d^3k}{(2\pi)^3}\left(\frac{k^2}{2m} + \epsilon^{BHF}(k)\right)\theta(k_F - k), \quad (5)$$

where $\rho = dk_F^3/3\pi^2$ is the density and d is the isospin degeneracy [$d=1(2)$ for PNM (SNM)]. The symmetry energy $S(\rho)$ is obtained as the difference between PNM and SNM energies for the same density.

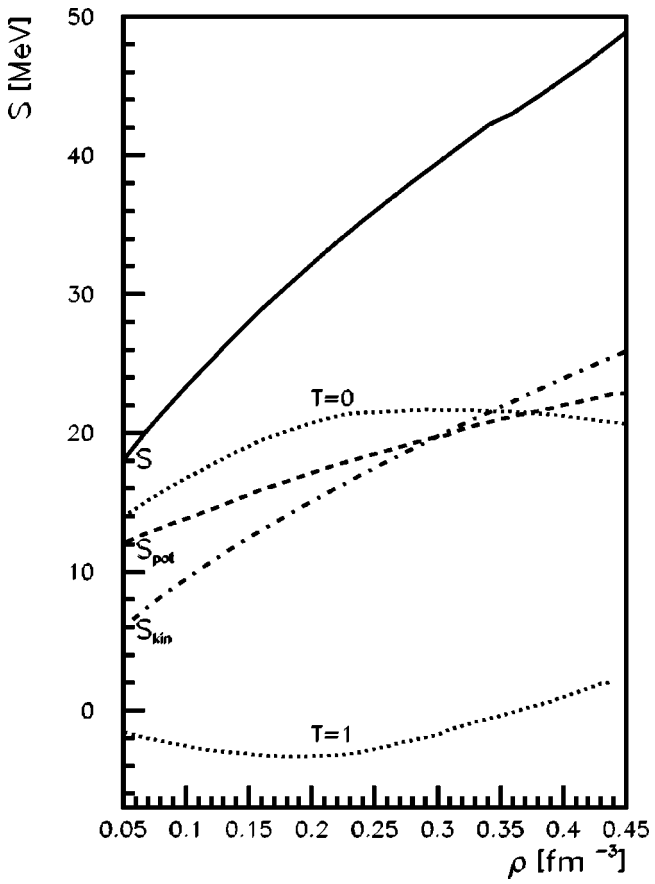

FIG. 1. The symmetry energy S (full line) and the contributions to S from the kinetic (dash-dotted line) and potential energy (dashed line), calculated within a ccBHF scheme and using the Reid93 interaction. Also shown (dotted lines) are the $T=0$ and $T=1$ components of the potential energy contribution.

We first performed ccBHF calculations with the Reid93 interaction, including partial waves with $J<4$ in the calculation of the G matrix. The results are presented in Fig. 1, where the symmetry energy S is decomposed into various contributions as suggested in Ref. [11] and shown as a function of nucleon density ρ.

The contribution S_{kin} of the kinetic energy to the BHF symmetry energy is given by the free Fermi-gas expression [1]

$$S_{\mathrm{kin}} = E_{kin,PNM} - E_{kin,SNM} = \frac{3}{10m}(3\pi^2)^{2/3}\rho^{2/3}\left(1 - \frac{1}{2^{2/3}}\right), \quad (6)$$

and it determines to a large extent the density dependence of S. In Fig. 1 we also show the symmetry potential $S_{\mathrm{pot}} = S - S_{\mathrm{kin}}$, which is much flatter, and the contributions to S_{pot} from both the isoscalar ($T=0$) and isovector ($T=1$) components of the interaction. Over the considered density range S_{pot} is dominated by the positive $T=0$ part. The $T=0$ partial waves, containing the tensor force in the $^3S_1 - {}^3D_1$ channel which gives a major contribution to the

[1] This expression differs from the standard one, which is based upon the derivative rather than the finite difference.

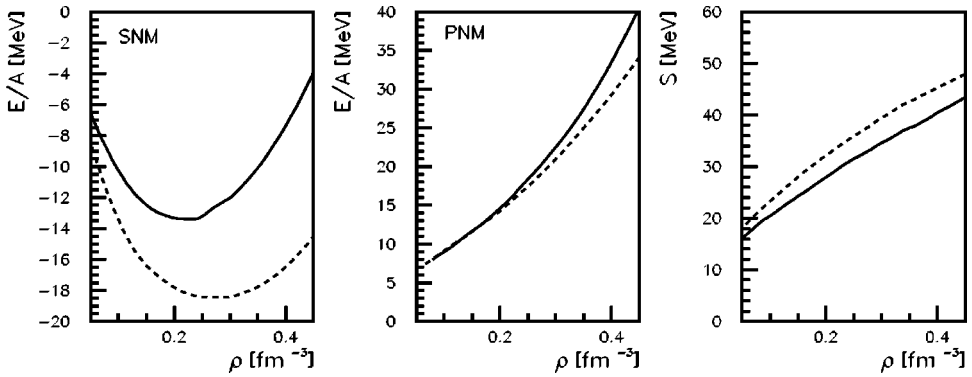

FIG. 2. The total energy per particle for symmetric nuclear matter (left panel) and pure neutron matter (central panel) for the Reid93 interaction. The dashed line refers to a ccBHF calculation, the full line to a SCGF calculation. The right panel displays the symmetry energy in these two approaches.

potential energy in SNM, do not contribute to the PNM energy. The $T=0$ contribution peaks at $\rho \approx 0.3$ fm^{-3}. The decrease of this contribution at higher densities is compensated by the increase of the $T=1$ potential energy, with as a net result a much weaker density dependence of the total potential energy. (It should be noted that inclusion of a three-nucleon interaction in general leads to a substantial increase for the slope parameter p_0 [12].)

2. Symmetry energy in SCGF approach

In recent years several groups have considered the replacement of the BBG hole-line expansion with the SCGF theory [16–21]. In Refs. [20,21] the binding energy for SNM was calculated within the SCGF framework and using the Reid93 potential. In the present paper we have extended these calculations to PNM and calculated the corresponding symmetry energy. Details of a technical nature can be found in Ref. [20].

A SCGF calculation differs in two important ways from a BHF calculation. First, within SCGF particles and holes are treated on an equal footing, whereas in BHF only intermediate particle ($k>k_F$) states are included in the ladder diagrams. This aspect ensures thermodynamic consistency, e.g., the Fermi energy or chemical potential of the nucleons equals the binding energy at saturation (i.e., it fulfills the Hugenholz–van Hove theorem). In the low-density limit BHF and SCGF coincide. As the density increases the phase space for hole-hole propagation is no longer negligible, and this leads to an important repulsive effect on the total energy. Second, the SCGF generates realistic spectral functions, which are used to evaluate the effective interaction and the corresponding nucleon self-energy. The spectral functions include a depletion of the quasiparticle peak and the appearance of single-particle strength at large values of energy and momentum, in agreement with experimental information from $(e,e'p)$ reactions. This is in contrast with the BHF approach where all the sp strength is concentrated at the BHF energy as determined from Eq. (4).

In a SCGF approach the particle states ($k>k_F$), which are absent in the BHF energy sum rule of Eq. (5), do contribute according to the energy sum rule

$$\frac{E}{A}=\frac{d}{\rho}\int\frac{d^3k}{(2\pi)^3}\int_{-\infty}^{\varepsilon_F}d\omega\left(\frac{k^2}{2m}+\omega\right)S_h(k,\omega), \qquad (7)$$

expressed in terms of the nucleon spectral function $S_h(k,\omega)$.

The results for the ccBHF and SCGF calculations for both SNM and PNM are compared in the left and central panels of Fig. 2 for the Reid93 interaction. The inclusion of high-momentum nucleons leads roughly to a doubling of the kinetic and potential energy in SNM, as compared to BHF. As seen in Fig. 2, the net result for the total energy of SNM is a repulsive effect, increasing with density [20]. This leads to a stiffer equation of state, and a shift of the SNM saturation density towards lower densities. The above effects are dominated by the tensor force (the isoscalar $^3S_1-^3D_1$ partial wave). Consequently, the effects are much smaller in PNM.

The corresponding symmetry energy, shown in the right panel of Fig. 2, is dominated by the shift in the total energy for SNM, and lies below the ccBHF symmetry energy in the entire density range. At $\rho_0=0.16$ fm^{-3} the symmetry energy parameter a_4 is reduced from 28.9 MeV to 24.9 MeV, while the slope p_0 remains almost the same (from 2.11 MeV fm^{-3} to 1.99 MeV fm^{-3}).

B. Comparison of symmetry energy in other approaches

1. Calculations with realistic NN forces

Engvik *et al.* [10] have performed lowest-order Brueckner-Hartree-Fock (LOBHF) calculations in SNM and PNM for all "modern" potentials (CD Bonn, Argonne v18, Reid93, Nijmegen I and II), which fit the Nijmegen *NN* scattering database with high accuracy. They concluded that for small and normal densities the symmetry energy is largely independent of the interaction used, e.g., at ρ_0 the values of S vary around an average value of $a_4=29.83$ MeV by about 1 MeV. At larger densities the spread becomes larger; however, the symmetry energy keeps increasing with density, in contrast to some of the older potentials such as Argonne v14 and the original Reid interaction (Reid68) for which $S(\rho)$ tended to saturate at densities larger than $\rho=0.4$ fm^{-3}. Some insight into the microscopic origin of the symmetry potential was obtained by Zuo *et al.* [11] who decomposed the symmetry energy into contributions from kinetic and potential energy. The BHF calculations in Ref. [11] used the Argonne v14 and the separable Paris interaction. In Fig. 1 we showed that the use of the modern Reid93 potential leads to essentially the same conclusions.

Detailed studies for SNM and PNM using variational chain summation techniques were performed by Wiringa *et al.* [22] for the Argonne Av14 and Urbana Uv14 *NN* interaction, in combination with the Urbana UVIII three-nucleon

TABLE I. Results for the symmetry energy parameters a_4 and p_0 from the variational calculations of Refs. [22,23] using the Argonne and Urbana *NN* potentials, in combination with Urbana models for the three-nucleon interaction. The last column includes a relativistic boost correction δv and the adjusted UIX* three-nucleon interaction.

	Av14	Av14+UVIII	Uv14	Uv14+UVIII	Av18	Av18+UIX	Av18+δv+UIX*
a_4 (MeV)	24.90	27.49	26.39	28.76	26.92	29.23	30.1
p_0 (MeV fm)$^{-3}$	2.02	2.71	2.38	3.04	1.95	3.24	2.95

interaction (TNI), and by Akmal *et al.* [23] for the modern Av18 *NN* potential in combination with the UIX-TNI. Results for a_4 and p_0, extracted from Refs. [22] and [23], are shown in Table I. The inclusion of TNI stiffens the EOS for both SNM and PNM, and increases considerably the value of the symmetry energy a_4 and its slope p_0 at the empirical density ρ_0. The effect of including a relativistic boost correction δv (in combination with a refitted TNI) on the values of a_4 and p_0 is sizable as well.

The symmetry energy has also been computed in the Dirac-Brueckner-Hartree-Fock approach [24,25]. In relativistic approaches the symmetry energy generally is found to increase almost linearly with density, and more rapidly than in the nonrelativistic case. This difference can be attributed to two effects. First the covariant kinetic energy which is inversely proportional to $\sqrt{k_F^2+m^{*2}}$ is larger because of the decreasing Dirac mass m^* with increasing density. Second the contribution from ρ exchange appears to be larger than in the nonrelativistic case [24].

2. Mean-field approach using effective interactions

Since the Furnstahl relation has been verified mainly in terms of mean-field models we discuss some results obtained in these approaches, which in general are based upon a parametrized effective interaction.

Brown [5] has investigated proton and neutron radii in terms of the nonrelativistic Skyrme Hartree-Fock (SHF) model. First he noted that a certain combination of parameters in the SHF is not determined well by a fit to ground-state binding energies, and that a wide range of predictions for the EOS for PNM is obtained. He also pointed out a direct correlation between the derivative of the neutron matter EOS (i.e., basically the symmetry energy coefficient p_0) and the neutron skin in ^{208}Pb.

Covariant approaches are in general based upon either a covariant Lagrangian with σ, ω, and ρ exchange (and possibly other mesons) [26,27], or on the use of contact interactions [2], solved as an energy density functional in the Hartree-Fock approximation. Sets of model parameters are determined by fitting bound state properties of nuclei. Specifically the isovector degree of freedom is determined by the exchange of isovector mesons; in case of ρ meson exchange the (positive definite) contribution to S is given by

$$a_4 = \frac{k_F^2}{6\sqrt{m^{*2}+k_F^2}} + \frac{g_\rho^2}{8m_\rho^2}\rho_0, \tag{8}$$

and its potential energy contribution to p_0, which scales with that for a_4, is $g_\rho^2/8m_\rho^2$ [2]. Typical values obtained for p_0 are around 4–6 MeV fm^{-3}, and $a_4 \sim 30-36$ MeV, i.e., considerably larger than in nonrelativistic approaches (a large part of the enhancement can be ascribed to the fact that the kinetic contribution is larger, because $m^* < m$). Recently in Refs. [28,29] this approach was extended by inclusion of the isovector-scalar partner δ of the isoscalar scalar σ meson. Because of the presence of the Lorentz factor m^*/E in the scalar potential contribution, $\sim -(g_\delta^2/8m_\delta^2)(m^*/E)$, which decreases with increasing density its inclusion leads to an even larger net value for p_0 [28,29].

Since explicit pion exchange is usually not included in the mean-field approaches it is difficult to make a meaningful comparison with microscopic ones. In fact it can be argued that in contrast to isoscalar properties the long-range pion exchange could play an essential role in determining the isovector properties [2].

3. Effective field theory

Recently the density dependence of the symmetry energy has been computed in chiral perturbation effective field theory, described by pions plus one cutoff parameter, Λ, to simulate the short distance behavior [30]. The nuclear matter calculations have been performed up to three-loop order; the resulting EOS is expressed as an expansion in powers of k_F, and the value of $\Lambda \approx 0.65$ GeV is adjusted to the empirical binding energy per nucleon. The value obtained in this approach for $a_4 = 33$ MeV is in remarkable agreement with the empirical one; at higher densities ($\rho > 0.2$ fm^{-3}) a downward bending is predicted. However, in its present form the validity of this approach is clearly confined to relatively small values of the Fermi momentum, i.e., rather low densities. It is interesting to note that there are relatively small (large) contributions to a_4 coming from one-pion exchange Fock diagram (three-loop diagrams with either two or three medium insertions).

4. Comparison

To summarize the present status in Fig. 3 various results of the approaches for $S(\rho)$ discussed above are compared. As noted above one sees that the covariant models yield a much larger increase of S with the density than the nonrelativistic approaches. The LOBHF leads to a higher value of S than both variational and the SCGF method which include more correlations; that the SCGF result is close to the variational approach may be fortuitous. Effects from three-body forces are not included.

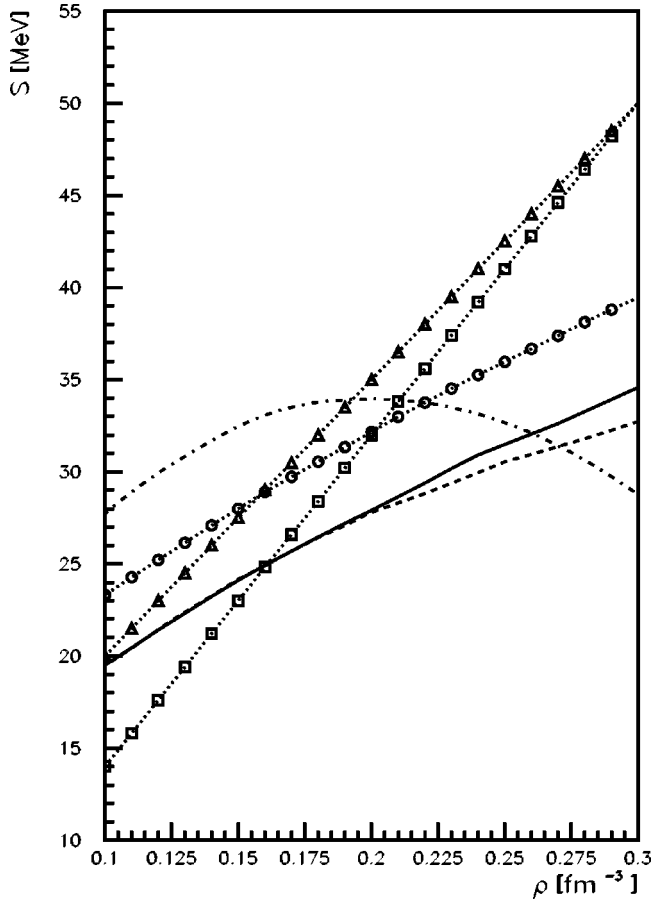

FIG. 3. Overview of several theoretical predictions for the symmetry energy S: Brueckner-Hartree-Fock (continuous choice) with Reid93 potential (circles), self-consistent Green function theory with Reid93 potential (full line), variational calculation from Ref. [22] with Argonne Av14 potential (dashed line), Dirac-Brueckner-Hartree-Fock calculation from Ref. [24] (triangles), relativistic mean-field model from Ref. [28] (squares), effective field theory from Ref. [30] (dash-dotted line).

III. RELATIONSHIP BETWEEN SYMMETRY ENERGY AND ΔR

Brown [5] and Furnstahl [2] have pointed out that within the framework of mean-field models there exists an almost linear empirical correlation between theoretical predictions for both a_4 and its density dependence p_0 and the neutron skin $\Delta R = R_n - R_p$ in heavy nuclei. This observation suggests an intriguing relationship between a bulk property of infinite nuclear matter and a surface property of finite systems.

Here we wish to address this question from a different point of view, namely in the spirit of Landau-Migdal approach. Let us consider a simple mean-field model (see, e.g., Ref. [31]) with the Hamiltonian consisting of the single-particle mean-field part $\hat{H}_0$ and the residual particle-hole interaction $\hat{H}_{p\text{-}h}$:

$$\hat{H} = \hat{H}_0 + \hat{H}_{p\text{-}h}, \quad \hat{H}_0 = \sum_a [T_a + U(x_a)], \tag{9}$$

$$U(x) = U_0(x) + U_1(x) + U_C(x), \tag{10}$$

$$U_0(x) = U_0(r) + U_{so}(x);\ U_1(x) = \frac{1}{2} S_{\rm pot}(r)\tau^{(3)};$$

$$U_C(x) = \frac{1}{2} U_C(r)(1 - \tau^{(3)}), \quad x = (r, \sigma, \tau).$$

Here, the mean-field potential $U(x)$ includes the phenomenological isoscalar part $U_0(x)$ along with the isovector $U_1(x)$ and the Coulomb $U_C(x)$ parts calculated consistently in the Hartree approximation; $U_0(r)$ and $U_{so}(x) = U_{so}(r)\vec{\sigma}\cdot\vec{l}$ are the central and spin-orbit parts of the isoscalar mean field, respectively; $S_{\rm pot}(r)$ is the symmetry potential (the potential part of the symmetry energy).

In the Landau-Migdal approach the effective isovector particle-hole interaction $\hat{H}_{p\text{-}h}$ is given by

$$\hat{H}_{p\text{-}h} = \sum_{a>b} (F' + G'\vec{\sigma}_a\vec{\sigma}_b)\vec{\tau}_a\vec{\tau}_b\delta(\vec{r}_a - \vec{r}_b), \tag{11}$$

where F' and G' are the phenomenological Landau-Migdal parameters.

The model Hamiltonian $\hat{H}$ in Eq. (10) preserves isospin symmetry if the condition

$$[\hat{H}, \hat{T}^{(-)}] = \hat{U}_C^{(-)} \tag{12}$$

is fulfilled, where $\hat{T}^{(-)} = \Sigma_a \tau_a^{(-)}$, $\hat{U}_C^{(-)} = \Sigma_a U_C(r_a)\tau_a^{(-)}$. With the use of Eqs. (10)–(12) the condition, Eq. (12), in the random phase approximation formalism leads to a self-consistency relation between the symmetry potential and the Landau parameter F' [32]:

$$S_{\rm pot}(r) = 2F' n^{(-)}(r), \tag{13}$$

where $n^{(-)}(r) = n^n(r) - n^p(r)$ is the neutron excess density. Thus, in this model the depth of the symmetry potential is controlled by the Landau-Migdal parameter F' (analogously to the role played by the parameter g_ρ^2 in relativistic mean-field models).

$S_{\rm pot}(r)$ is obtained from Eq. (13) by an iterative procedure; the resulting dependence of ΔR on the dimensionless parameter $f' = F'/(300\ \text{MeV fm})^3$ shown in Fig. 4 indeed illustrates that ΔR depends almost linearly on f'. Then with the use of the Migdal relation [33] which relates symmetry energy and f',

$$a_4 = \frac{\epsilon_F}{3}(1 + 2f'), \tag{14}$$

a similar almost linear correlation between the symmetry energy a_4 and the neutron skin is obtained.

To get more insight in the role of f' we consider small variations $\delta F'$. Neglecting the variation of $n^{(-)}(r)$ with respect to $\delta F'$ one has a linear variation of the symmetry potential: $\delta S_{\rm pot}(r) = 2\delta F' n^{(-)}(r)$. Then in first-order perturbation theory, such a variation of $S_{\rm pot}$ causes the following variation of the ground-state wave function:

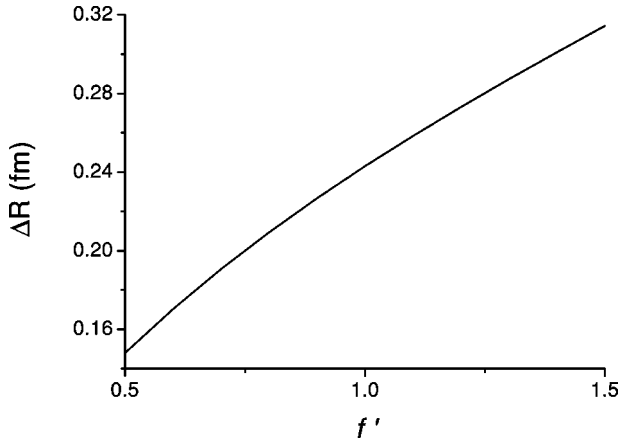

FIG. 4. Neutron skin in ^{208}Pb vs the Landau-Migdal parameter f'.

$$|\delta 0\rangle = \delta F' \sum_s \frac{\langle s|\hat{N}^{(-)}|0\rangle}{E_0 - E_s}|s\rangle, \tag{15}$$

with s labeling the eigenstates of the nuclear Hamiltonian and a single-particle operator $\hat{N}^{(-)}=\Sigma_a n^{(-)}(r_a)\tau_a^{(3)}$. Consequently the variation of the expectation value of the single-particle operator $\hat{V}^{(-)}=\Sigma_a r_a^2\tau_a^{(3)}$ with $\langle 0|\hat{V}^{(-)}|0\rangle = NR_n^2 - ZR_p^2$ can be written as

$$R_p\delta(\Delta R) = \delta F' \frac{2}{A}\sum_s \frac{\mathrm{Re}\langle 0|\hat{N}^{(-)}|s\rangle\langle s|\hat{V}^{(-)}|0\rangle}{E_0 - E_s}. \tag{16}$$

In practice the sum in Eq. (16) is exhausted mainly by the isovector monopole resonance of which the high excitation energy (about 24 MeV in ^{208}Pb) justifies the perturbative consideration. We checked that Eq. (16) is able to reproduce directly calculated $\delta(\Delta R)$ shown in Fig. 4 with the accuracy of about 10%. As a result a simple microscopic interpretation of the linear correlation between the neutron skin thickness and Landau parameter F' is obtained.

IV. EXPERIMENTAL METHODS TO DETERMINE ΔR

A variety of experimental approaches have been explored in the past to obtain information on ΔR. To a certain extent all analyses contain a certain model dependence, which is difficult to estimate quantitatively. It is not our intention to present a full overview of existing methods for the special case of ^{208}Pb. In particular the results obtained in the past from the analysis of elastic proton and neutron scattering have varied depending upon specifics of the analysis employed. At present the most accurate value comes from a recent detailed analysis of the elastic proton scattering reaction at E=0.5–1 GeV [34], and of neutron and proton scattering at E=40–100 MeV [35]. For details we refer to these papers. Here we restrict ourselves to a discussion of some less well-known methods that have the potential to provide more accurate information on the neutron skin in the future. In particular the excitation of isovector giant resonances through the restoring force contains information about the symmetry energy.

A. Isovector giant resonances

We begin with a brief overview of the study of excitation of isovector giant resonances. Sum rules for the latter contain direct information on ΔR.

1. Giant dipole resonance (GDR)

In the past the excitation of the isovector giant dipole resonance (GDR) with isoscalar probes has been used to extract $\Delta R/R$ [36]. In the distorted wave Born approximation optical model analysis of the cross section the neutron and proton transition densities are needed as an input. In the Goldhaber-Teller picture,

$$g_i(r) = -\kappa\frac{2N_i}{A}\frac{d\rho_i}{dr} \tag{17}$$

with κ the oscillation amplitude and $(i=p,n)$. We assume ground-state neutron and proton distributions of the form $[x=(N-Z)/A]$

$$\rho_i(r) = \frac{1}{2}(1 \pm x \mp \gamma x)\rho[r - c(1 \pm \gamma x/3)]. \tag{18}$$

While for $N=Z$ the transition density vanishes, for $N>Z$ the isovector transition density is finite,

$$\Delta g(r) = \kappa\gamma\frac{N-Z}{A}\left(\frac{d\rho}{dr} + \frac{c}{3}\frac{d^2\rho}{dr^2}\right),$$

where γ is related to ΔR, $\gamma=[3A/2(N-Z)]\Delta R/R_0$.

Excitation of the GDR by α particle scattering (isoscalar probe) the corresponding transition optical potential is given by

$$\Delta U_{tr} = \kappa\gamma\frac{N-Z}{A}\left(\frac{dU}{dr} + \frac{R_0 d^2U_0}{3dr^2}\right). \tag{19}$$

By comparing the experimental cross section with the theoretical one (calculated as a function of the ratio $\Delta R/R$) the value of $\Delta R/R$ can be deduced.

It is difficult to make a quantitative estimate of the uncertainty in the result coming from the model dependence of the approach. In the analysis several assumptions must be made, such as the radial shape of the density oscillations and about the actual values of the optical model parameters.

2. Spin-dipole giant resonance

Recently it has been proposed to utilize the excitation of the spin-dipole resonance (SDR), excited in charge exchange reactions, to determine the neutron skin; in fact the method has been applied to obtain information on the variation of the neutron skin in the Sn isotopes with isotope number [37]. For the relevant operator $\Sigma\sigma_i\tau_i^{\pm}r_iY_1(r_i)$, the summed ΔL=1 strength is

$$S^{(-)} - S^{(+)} = C(NR_n^2 - ZR_p^2). \quad (20)$$

Here $S^{(-)}$ and $S^{(+)}$ are the spin-dipole total strengths in $\beta^{(-)}$ and $\beta^{(+)}$ channels, respectively; C is the factor depending on the definition of the spin-dipole operator (in the definition of Ref. [2] $C=1/4\pi$, we use here $C=1$). Because $S^{(+)}$ could not be measured experimentally, the model-dependent energy-weighted sum rule was invoked in the analysis to eliminate $S^{(+)}$. Let us put $S^{(+)}=0$ (that seems to be a very good approximation for ^{208}Pb) and ask the question what experimental accuracy for $S^{(-)}$ is needed to determine the neutron skin to a given accuracy. With

$$S^{(-)} = (N-Z)R_p^2 + 2NR_p\Delta R \quad (21)$$

the ratio of the second term on the right-hand side to the first one in case of ^{208}Pb is

$$2N\Delta R/[(N-Z)R_p] \approx 5.7\Delta R/R_p.$$

Therefore, for $R_p=5.5$ fm and $\Delta R=0.2$ fm the second term is only 25% of the first one and one needs 3% accuracy in $S^{(-)}$ to determine ΔR with 10% accuracy. Because the SDR strength is spread out and probably has a considerable strength at low energy the results for the ΔR can be only considered as qualitative with a relatively large uncertainty (of the order of 30–50%).

3. Isobaric analog state

The dominant contribution to the energy-weighted sum rule (EWSR) for Fermi excitations by the operator $T^{(-)}$ comes from the Coulomb mean field [38]

$$(\mathrm{EWSR})_F = \int U_C(r)n^{(-)}(r)d^3r. \quad (22)$$

The Coulomb mean field $U_C(r)$ resembles very much that of the uniformly charged sphere, being inside a nucleus a quadratic function: $U_C(r)=(Ze^2/2R_c)[3-(r/R_c)^2]$, $r\leqslant R_c$. It turns out that if one extends such a quadratic dependence also to the outer region $r>R_c$ (instead of proportionality to R_c/r), it gives numerically just very small deviation in $(\mathrm{EWSR})_F$ [less than 0.5%, due to the fact that the difference and its first derivative go to 0 at $r=R_c$ and $n^{(-)}(r)$ is exponentially decreasing at $r>R_c$]. Using such an approximation, one gets

$$(\mathrm{EWSR})_F \approx (N-Z)\Delta_C\left(1-\frac{S^{(-)}}{3(N-Z)R_c^2}\right) \quad (23)$$

with $\Delta_C=3Ze^2/2R_c$, and $S^{(-)}$ given in Eq. (21).

Since the isobaric analog state (IAS) exhausts almost 100% of the non-EWSR and EWSR, one may hope to extract $S^{(-)}$ from the IAS energy. However, the term depending on $S^{(-)}$ contributes only about 20% to $(\mathrm{EWSR})_F$, and as a result, the part of $S^{(-)}$ depending on ΔR contributes only about 4% to $(\mathrm{EWSR})_F$ (in ^{208}Pb). From the experimental side, the IAS energy can be determined with unprecendently high accuracy, better than 0.1%. Also, from the experimentally known charge density distribution the Coulomb mean field $U_C(r)$ can be calculated rather accurately, and hence one can determine the small difference between Eqs. (23) and (22). But at the level of 1% accuracy several theoretical effects discarded in Eq. (22) come into play (see, e.g., Ref. [38]) which makes the reliability of such a method questionable. On the other hand in a forthcoming paper we will show that for an isotopic chain the excitation of the IAS can be used as a quantitative tool to obtain the variation of ΔR with neutron number.

B. Antiprotonic atoms

Recently neutron density distributions were deduced from antiprotonic atoms [39]. The basic method determines the ratio of neutron and proton distributions at large differences by means of a measurement of the annihilation products which indicates whether the antiproton was captured on a neutron or a proton. In the analysis two assumptions are made. First, a best fit value for the ratio R_I of the imaginary parts of the free space $\bar{p}p$ and $\bar{p}n$ scattering lengths equal to unity is adopted. Second, in order to reduce the density ratio at the annihilation side to a ratio of rms radii a two-parameter Fermi distribution is assumed. The model dependence introduced by this assumption is difficult to judge. Since a large number of nuclei have been measured one may argue that the value of R_I is fixed empirically.

C. Parity violating electron scattering

Recently it has been proposed to use the (parity violating) weak interaction to probe the neutron distribution. This is probably the least model-dependent approach [41]. The weak potential between electron and a nucleus is

$$\tilde{V}(r) = V(r) + \gamma_5 A(r), \quad (24)$$

where the axial potential $A(r)=(G_F/2^{3/2})\rho_W(r)$. The weak charge is mainly determined by neutrons

$$\rho_W(r) = (1-4\sin^2\theta_W)\rho_p(r) - \rho_n(r), \quad (25)$$

with $\sin^2\theta_W \approx 0.23$. In a scattering experiment using polarized electrons one can determine the cross section asymmetry [41] which comes from the interference between the A and V contributions. Using the measured neutron form factor at small finite value of Q^2 and the existing information on the charge distribution one can uniquely extract the neutron skin. Some slight model dependence comes from the need to assume a certain radial dependence for the neutron density, to extract R_n from a finite Q^2 form factor.

V. DISCUSSION OF ΔR FOR ^{208}Pb AND SOME IMPLICATIONS

In Table II we present a summary of some recent results on ΔR in ^{208}Pb. One sees that (with the exception of the analysis of proton and neutron pickup reactions in terms of mean-field orbitals in Ref. [42]) all recent results are consistent with $\Delta R \sim 0.13 \pm 0.03$ fm. Therefore it appears that the data agree with the result of conventional Skyrme model approach but seem to disagree with the results of the RMF models considered in Ref. [2]. One the basis of the correla-

TABLE II. Summary of recent results for ΔR in ^{208}Pb.

Method	ΔR(fm)	Error (fm)	Ref.
Giant dipole resonance excitation	0.19	0.09	[36,40]
Neutron/proton pickup	0.51		[42]
$(\vec{p}, p')$ at 0.5–1.04 GeV	0.097	0.014	[34]
Nucleon scattering (40–200 MeV)	0.17		[35]
Antiprotonic atoms	0.15	0.02	[39]
Parity violating electron scattering	Planned	0.05	[41]

tion plot between ΔR and p_0 shown in Ref. [2] one would then conclude that a small value for $p_0 \sim 2$ MeV/fm^3 is preferred over larger values predicted in RNF approaches.

In several processes of physical interest knowledge of ΔR plays a crucial role and in fact a more accurate value could lead to more stringent tests.

(i) The pion polarization operator [8] (the *s*-wave optical potential) in a heavy nucleus, $\Pi(\omega, \rho_p, \rho_n) = -T^+(\omega)\rho - T^-(\omega)(\rho_n - \rho_p)$, has mainly an isovector character $[T^+(m_\pi) \sim 0]$. Parametrizing the densities by Fermi shapes for the case of ^{208}Pb the main nuclear model dependence in the analysis comes from the uncertainty in the value of ΔR multiplying T^-.

(ii) Parity violation in atoms is dominated by *Z*-boson exchange between the electrons and the neutrons [9,44]. Taking the proton distribution as a reference there is a small so-called neutron skin (ns) correction to the parity nonconserving amplitude, $\delta E^{\rm ns}_{\rm pnc}$, for, say, a $6s_{1/2} \rightarrow 7s_{1/2}$ transition, which is related to ΔR as [44] (independent of the electronic structure)

$$\frac{\delta E^{\rm ns}_{\rm pnc}}{E_{\rm pnc}} = -\frac{3}{7}(\alpha Z)^2 \frac{\Delta R}{R_p}. \tag{26}$$

In ^{133}Cs it amounts to a $\delta E/E \approx -(0.1-0.4)\%$ depending on whether the nonrelativistic or relativistic estimates for ΔR are used [9]. The corresponding uncertainty in the weak charge Q_W is $-(0.2-0.8)\sigma$.

(iii) The pressure in neutron star matter can be expressed as in terms of the symmetry energy and its density dependence [1]

$$P(\rho, x) = \rho^2 \frac{\partial E(\rho, x)}{\partial \rho} = \rho^2 [E'(\rho, 1/2) + S'(\rho)(1-2x)^2 + \ldots]. \tag{27}$$

By using the β equilibrium condition in a neutron star, $\mu_e = \mu_n - \mu_p = -\partial E(\rho, x)/\partial x$, and the result for the electron chemical potential, $\mu_e = 3/4\hbar c x (3\pi^2 \rho x)^{1/3}$, one finds the proton fraction near saturation density, ρ_0, to be quite small, $x_0 \sim 0.04$. Hence the pressure at saturation density can be approximated as

$$P(\rho_0) = \rho_0(1-2x_0)[\rho_0 S'(\rho_0)(1-2x_0) + S(\rho_0)x_0] \sim \rho_0^2 S'(\rho_0). \tag{28}$$

At higher densities the proton fraction increases; this increase is more rapid in case of larger p_0 [26]. While for the pressure at higher densities contributions from other nuclear quantities such as compressibility will play a role, in Ref. [1] it was argued that that there is a correlation of the neutron star radius and the pressure which does not depend on the EOS at the highest densities. Numerically the correlation can be expressed in the form of a power law, $R_M \sim C(\rho, M)[P(\rho)/\text{MeV fm}^{-3}]^{0.25}$ km, where $C(\rho = 1.5\rho_0, M = 1.4M_{solar}) \sim 7$. This shows that a determination of a neutron star radius would provide some constraint on the symmetry properties of nuclear matter.

VI. CONCLUSION

In this paper we have discussed the bulk symmetry energy, and compared various approaches to compute it as a function of density. Because the tensor interaction plays an important role the symmetry energy is sensitive to details of the treatment of the many-body correlations. It was shown that the self-consistent Green function approach in which more correlations are included than in lowest-order BHF leads to a smaller value of the symmetry energy. The relatively large values for p_0 obtained in the relativistic mean-field approach can be associated with an effective mass effect.

We showed that the phenomenological almost linear relationship between symmetry energy and neutron skin in finite nuclei observed in mean-field calculations could be understood in terms of the Landau-Migdal approach. Finally we compared several experimental tools of potential interest for the determination of the neutron skin.

ACKNOWLEDGMENTS

This work was part of the research program of the "Stichting voor Fundamenteel Onderzoek der Materie" (FOM) with financial support from the "Nederlandse Organisatie voor Wetenschappelijk Onderzoek" (NWO). Y.D. acknowledges support from FWO-Vlaanderen. The authors would like to thank Professor M. Urin for several clarifying remarks.

[1] J. M. Lattimer and M. Prakash, Astrophys. J. **550**, 426 (2001); astro-ph/0002232.
[2] R. J. Furnstahl, Nucl. Phys. **A706**, 85 (2002).
[3] B. A. Li, C. M. Ko, and W. Bauer, Int. J. Mod. Phys. E **7**, 147 (1998).
[4] Bao-An Li, Phys. Rev. Lett. **88**, 192701 (2002); Nucl. Phys. **A708**, 365 (2002).
[5] B. A. Brown, Phys. Rev. Lett. **85**, 5296 (2000).
[6] A. R. Bodmer and Q. N. Usmani, Phys. Rev. C **67**, 034305 (2003).

[7] C. J. Horowitz and J. Piekarewicz, Phys. Rev. Lett. **86**, 5647 (2001).
[8] E. E. Kolomeitsev, N. Kaiser, and W. Weise, Phys. Rev. Lett. **90**, 092501 (2003).
[9] S. J. Pollock and M. C. Welliver, Phys. Lett. B **464**, 177 (1998).
[10] L. Engvik, M. Hjorth-Jensen, R. Machleidt, H. Müther, and A. Polls, Nucl. Phys. **A627**, 85 (1997).
[11] W. Zuo, I. Bombaci, and U. Lombardo, Phys. Rev. C **60**, 024605 (1999).
[12] W. Zuo *et al.*, Eur. Phys. J. A **14**, 469 (2002).
[13] K. Oyamatsu *et al.*, Nucl. Phys. **A634**, 3 (1998).
[14] M. Baldo, G. Giansiracusa, U. Lombardo, and H. Q. Song, Phys. Lett. B **473**, 1 (2000).
[15] M. Baldo, A. Fiasconaro, H. Q. Song, G. Giansiracusa, and U. Lombardo, Phys. Rev. C **65**, 017303 (2001).
[16] A. Ramos, A. Polls, and W. H. Dickhoff, Nucl. Phys. **A503**, 1 (1989).
[17] P. Bozek, Phys. Rev. C **65**, 054306 (2002); Eur. Phys. J. A **15**, 325 (2002); P. Bozek and P. Czerski, *ibid.* **11**, 271 (2001).
[18] W. H. Dickhoff and E. P. Roth, Acta Phys. Pol. B **33**, 65 (2002).
[19] Y. Dewulf, D. Van Neck, and M. Waroquier, Phys. Lett. B **510**, 89 (2001).
[20] Y. Dewulf, D. Van Neck, and M. Waroquier, Phys. Rev. C **65**, 054316 (2002).
[21] Y. Dewulf, W. H. Dickhoff, D. Van Neck, E. R. Stoddard, and M. Waroquier, Phys. Rev. Lett. **90**, 152501 (2003).
[22] R. B. Wiringa, V. Fiks, and A. Fabrocini, Phys. Rev. C **38**, 1010 (1988).
[23] A. Akmal, V. R. Pandharipande, and D. G. Ravenhall, Phys. Rev. C **58**, 1804 (1998).
[24] C.-H. Lee, T. T. S. Kuo, G. Q. Li, and G. E. Brown, Phys. Rev. C **57**, 3488 (1998).
[25] K. Sumiyoshi, K. Oyamatsu, and H. Toki, Nucl. Phys. **A595**, 327 (1995).
[26] C. J. Horowitz and J. Piekarewicz, Phys. Rev. C **66**, 055803 (2002).
[27] P. Ring, Prog. Part. Nucl. Phys. **37**, 193 (1996), and references therein.
[28] B. Liu *et al.*, Phys. Rev. C **65**, 045201 (2002).
[29] V. Greco *et al.*, Phys. Rev. C **67**, 015203 (2003).
[30] N. Kaiser, S. Fritsch, and W. Weise, Nucl. Phys. **A697**, 255 (2002).
[31] M. L. Gorelik, S. Shlomo, and M. H. Urin, Phys. Rev. C **62**, 044301 (2000).
[32] B. L. Birbrair and V. A. Sadovnikova, Sov. J. Nucl. Phys. **20**, 347 (1975); O. A. Rumyantsev and M. H. Urin, Phys. Rev. C **49**, 537 (1994).
[33] A. B. Migdal, *Theory of Finite Fermi Systems and Applications to Atomic Nuclei* (Interscience, London, 1967).
[34] B. C. Clark, L. J. Kerr, and S. Hama, Phys. Rev. C **67**, 054605 (2003).
[35] S. Karataglidis, K. Amos, B. A. Brown, and P. K. Deb, Phys. Rev. C **65**, 044306 (2002).
[36] A. Krasznahorkay *et al.*, Nucl. Phys. **A567**, 521 (1994).
[37] A. Krasznahorkay *et al.*, Phys. Rev. Lett. **82**, 3216 (1999).
[38] N. Auerbach, J. Huefner, A. K. Kerman, and C. M. Shakin, Rev. Mod. Phys. **44**, 48 (1972).
[39] A. Trzcinska *et al.*, Phys. Rev. Lett. **87**, 082501 (2001).
[40] A. Krasznahoray (private communication).
[41] C. Horowitz *et al.*, Phys. Rev. C **63**, 025501 (2001).
[42] G. Mairle and G. Grabmayr, Eur. Phys. J. A **9**, 313 (2000).
[43] L. Ray, G. W. Hoffmann, and W. R. Coker, Phys. Rep. **212**, 223 (1992).
[44] A. Derevianko, Phys. Rev. A **65**, 012106 (2002).